Year: 2019

Commonality despite exceptional diversity in the baseline human antibody repertoire

Briney, Bryan ; Inderbitzin, Anne ; Joyce, Collin ; Burton, Dennis R

Abstract: In principle, humans can produce an antibody response to any non-self-antigen molecule in the appropriate context. This flexibility is achieved by the presence of a large repertoire of naive antibodies, the diversity of which is expanded by somatic hypermutation following antigen exposure[1]. The diversity of the naive antibody repertoire in humans is estimated to be at least 10^{12} unique antibodies[2]. Because the number of peripheral blood B cells in a healthy adult human is on the order of 5×10^9, the circulating B cell population samples only a small fraction of this diversity. Full-scale analyses of human antibody repertoires have been prohibitively difficult, primarily owing to their massive size. The amount of information encoded by all of the rearranged antibody and T cell receptor genes in one person-the 'genome' of the adaptive immune system-exceeds the size of the human genome by more than four orders of magnitude. Furthermore, because much of the B lymphocyte population is localized in organs or tissues that cannot be comprehensively sampled from living subjects, human repertoire studies have focused on circulating B cells[3]. Here we examine the circulating B cell populations of ten human subjects and present what is, to our knowledge, the largest single collection of adaptive immune receptor sequences described to date, comprising almost 3 billion antibody heavy-chain sequences. This dataset enables genetic study of the baseline human antibody repertoire at an unprecedented depth and granularity, which reveals largely unique repertoires for each individual studied, a subpopulation of universally shared antibody clonotypes, and an exceptional overall diversity of the antibody repertoire.

DOI: https://doi.org/10.1038/s41586-019-0879-y

Originally published at:
Briney, Bryan; Inderbitzin, Anne; Joyce, Collin; Burton, Dennis R (2019). Commonality despite exceptional diversity in the baseline human antibody repertoire. Nature, 566(7744):393-397.
DOI: https://doi.org/10.1038/s41586-019-0879-y

https://doi.org/10.1038/s41586-019-0879-y

Commonality despite exceptional diversity in the baseline human antibody repertoire

Bryan Briney[1,2,3,4,5]*, Anne Inderbitzin[1,6], Collin Joyce[1,2,3,4] & Dennis R. Burton[1,2,4,5,7]*

In principle, humans can produce an antibody response to any non-self-antigen molecule in the appropriate context. This flexibility is achieved by the presence of a large repertoire of naive antibodies, the diversity of which is expanded by somatic hypermutation following antigen exposure[1]. The diversity of the naive antibody repertoire in humans is estimated to be at least 10^{12} unique antibodies[2]. Because the number of peripheral blood B cells in a healthy adult human is on the order of 5×10^9, the circulating B cell population samples only a small fraction of this diversity. Full-scale analyses of human antibody repertoires have been prohibitively difficult, primarily owing to their massive size. The amount of information encoded by all of the rearranged antibody and T cell receptor genes in one person—the 'genome' of the adaptive immune system—exceeds the size of the human genome by more than four orders of magnitude. Furthermore, because much of the B lymphocyte population is localized in organs or tissues that cannot be comprehensively sampled from living subjects, human repertoire studies have focused on circulating B cells[3]. Here we examine the circulating B cell populations of ten human subjects and present what is, to our knowledge, the largest single collection of adaptive immune receptor sequences described to date, comprising almost 3 billion antibody heavy-chain sequences. This dataset enables genetic study of the baseline human antibody repertoire at an unprecedented depth and granularity, which reveals largely unique repertoires for each individual studied, a subpopulation of universally shared antibody clonotypes, and an exceptional overall diversity of the antibody repertoire.

Eighteen sequencing libraries were generated for each of ten subjects (Extended Data Fig. 1). These libraries yielded 2.90×10^9 raw reads. After annotation[4], which included duplicate removal using unique molecular identifiers[5], we obtained 3.64×10^8 productive antibody sequences (Extended Data Table 1).

Amplification was reproducible, with similar gene usage between replicates (Fig. 1a, Extended Data Fig. 2). The frequencies of IgM-encoding (0.62–0.94) and IgG-encoding (0.06–0.38) sequences were consistent with the expected frequency of circulating B cells that express these isotypes[6] (Fig. 1b). Although V-gene, J-gene and CDRH3 length distributions were similar between subjects (Fig. 1c, e, f), differences were large enough that individual repertoires could conceivably be distinguished using only these features. We reduced sequence subsamples to the frequency distributions of V-gene, J-gene and CDRH3 length, and quantified similarity using the Morisita–Horn similarity index[7,8]. Subject repertoires were clearly distinguishable using as few as 10^4 sequences (Fig. 1d, Extended Data Fig. 4) and did not cluster by age, gender or ethnicity (Fig. 1g). The IgG^+ repertoires were least similar, suggesting that the unique immunological histories of subjects are a substantial contributor to repertoire individuality (Fig. 1h). A one-versus-rest support-vector-machine classifier trained on V-gene, J-gene and CDRH3 length data from 5 of the 6 biological replicates from each subject accurately assigned the remaining replicate using test or training datasets of as few as 500 sequences from each replicate (Fig. 1i).

To estimate repertoire diversity and minimize the effects of sequencing and amplification error, we first considered clonotype diversity. An antibody clonotype is a collection of sequences using the same V and J genes, and encoding an identical CDRH3 amino acid sequence[9]. For each subject, all sequences from each biological replicate were collapsed into a set of unique clonotypes. Any clonotypes that were repeatedly observed after pooling de-duplicated biological replicates must be derived from different cells, which provides a straightforward means of quantifying multiple occurrence. For clarity, clonotypes or sequences present in multiple biological replicates from a single subject will be referred to as 'repeatedly observed', whereas clonotypes or sequences found in multiple subjects will be referred to as 'shared'.

Rarefaction curves indicated a low frequency of repeatedly observed clonotypes, which is supported by capture–recapture sampling (3.9–11.7% recapture; Fig. 2a, Extended Data Fig. 6). To estimate repertoire diversity, we selected two estimators: Chao 2 and Recon. Chao 2 is a non-parametric estimator that uses repeat occurrence data from multiple samples to estimate species richness[10]. Recon uses maximum likelihood to estimate species richness, assuming only that the overall size of the repertoire is large (relative to sampling depth) and well-mixed[11]. These estimates represent the total diversity that the humoral immune system is capable of generating. Accordingly, these estimates may greatly exceed the actual number of B cells present in a single individual at any one time. The estimators produced similar estimates of clonotype diversity for each subject, with identical rank order (Fig. 2b). Recon consistently estimated about twofold greater repertoire diversity (2×10^7–1×10^9) than Chao 2 (1×10^7–5×10^8), consistent with reports that Chao 2 underestimates richness for samples with a non-negligible frequency of rare species[12,13]. Pooling unique clonotypes from multiple subjects enabled us to estimate cohort-wide diversity (Fig. 2c). Chao 2 (5×10^9) and Recon (5×10^9) produced nearly identical estimates for the complete ten-subject pool. Estimates of cohort-wide clonotype diversity exceed individual subject estimates by less than two orders of magnitude, which suggests a relatively high frequency of shared clonotypes. We next sought to estimate the sequence diversity for each individual, again using both the Chao 2 and Recon estimators (Fig. 2d). As expected, the estimates for sequences were substantially higher than for clonotypes, with Chao 2 (2×10^8–2×10^9) and Recon (1×10^8–2×10^9) producing comparable estimates for each subject. Unlike the cohort-wide clonotype estimates, Recon estimated much lower cohort-wide sequence diversity (1×10^{10}) than Chao 2 (1×10^{11}; Fig. 2e). The light-chain repertoire is estimated to be approximately four orders of magnitude less diverse than the heavy-chain repertoire (Extended Data Fig. 7) and pairing of heavy and light chains is approximately random[14], which produces a total paired-sequence diversity estimate of 10^{16} to 10^{18}. The most commonly cited estimate of antibody repertoire diversity—10^{12} unique sequences[2]—considers only the unmutated naive repertoire. As such,

[1]Department of Immunology and Microbiology, The Scripps Research Institute, La Jolla, CA, USA. [2]Center for HIV/AIDS Vaccine Immunology and Immunogen Discovery, The Scripps Research Institute, La Jolla, CA, USA. [3]Center for Viral Systems Biology, The Scripps Research Institute, La Jolla, CA, USA. [4]IAVI Neutralizing Antibody Center, The Scripps Research Institute, La Jolla, CA, USA. [5]Human Vaccines Project, New York, NY, USA. [6]Division of Infectious Diseases and Hospital Epidemiology, University Hospital Zurich, University of Zurich, Zurich, Switzerland. [7]Ragon Institute of MGH, MIT and Harvard, Cambridge, MA, USA. *e-mail: briney@scripps.edu; burton@scripps.edu

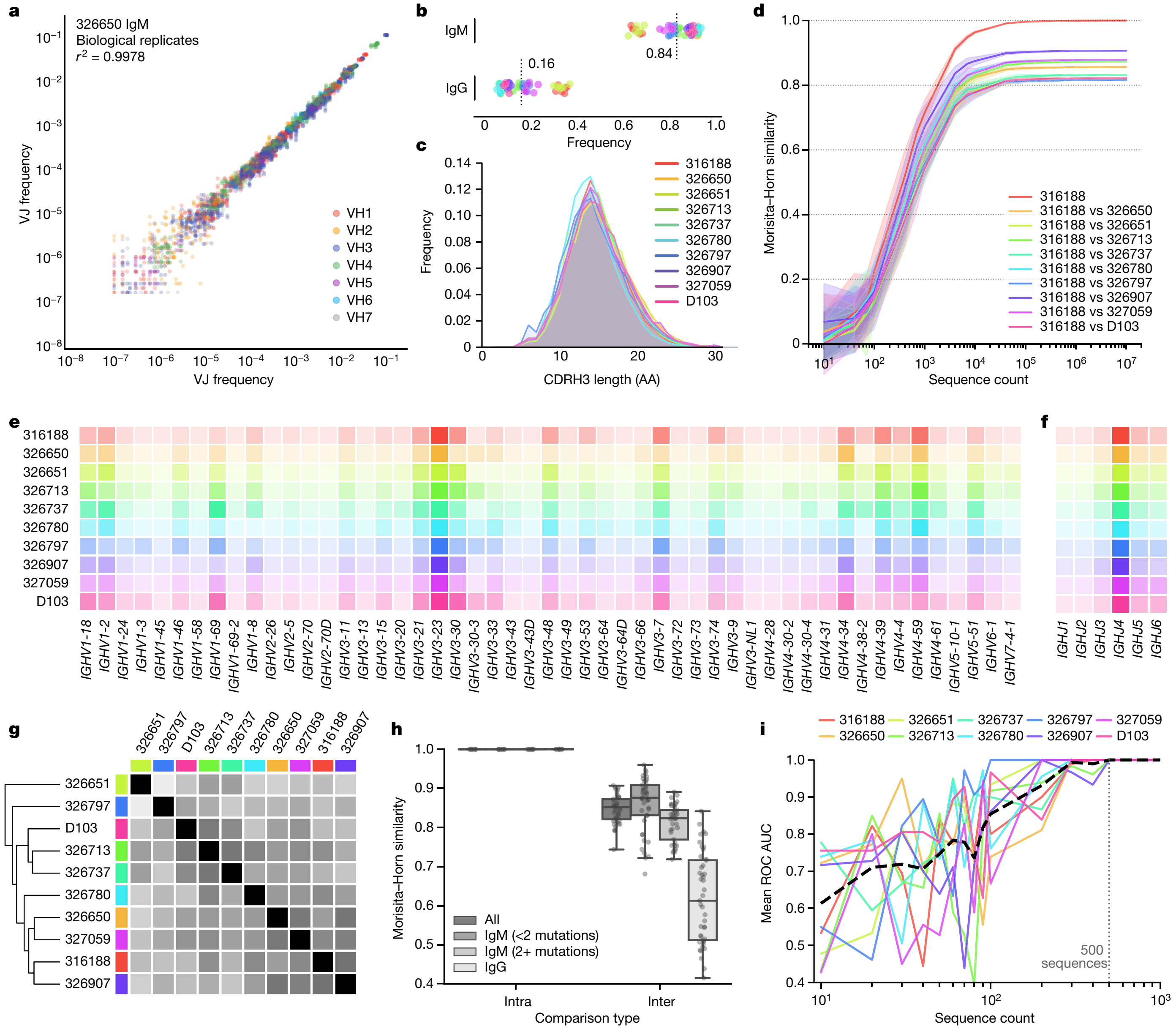

Fig. 1 | Uniqueness of the repertoires of individual subjects. **a**, Frequency comparison of V and J combinations in biological replicates from subject 326650. V and J combinations are coloured according to the V gene used. **b**, Sequence frequency by antibody isotype. Subjects are coloured as in **c**. Each point represents a single biological replicate. Mean of all samples is indicated for each isotype. **c**, CDRH3 length distribution for each subject. CDRH3 lengths were determined using the Immunogenetics (IMGT) numbering scheme. AA, amino acids. **d**, Morisita–Horn similarity of pairwise comparisons between subject 316188 and each of the other subjects. Lines indicate mean similarity of 20 bootstrap samplings, and shaded areas indicate 95% confidence intervals. Data from subject 316188 are representative; plots for all other subjects can be found in Extended Data Fig. 4. **e**, **f**, V gene (**e**) and J gene (**f**) use by subject. Increased colour intensity indicates higher frequency. Subjects are coloured as in **c**. **g**, Clustered distance matrix of subjects, using pairwise Morisita–Horn similarity of V-gene, J-gene and CDRH3 length as the distance measure. Distance matrix was computed using single-linkage clustering (Euclidean distance metric). Subject colours are as in **c**. A dendrogram representation of the distance matrix is also shown on the left side of the distance matrix. **h**, Comparison of intra- and inter-subject similarity in V-gene, J-gene and CDRH3 length, using all sequences, IgM sequences with fewer than two nucleotide mutations, IgM sequences with two or more mutations, or IgG sequences. Points represent individual intra- or inter-subject comparisons. Box plots show the median line and span the 25th–75th percentile, with whiskers indicating the 95% confidence interval. **i**, Mean receiver operating characteristic (ROC) area under the curve (AUC) for a one-versus-rest support-vector-machine classifier. The ROC AUC does not drop below 1.0 for any subject when the test or training datasets include ≥ 500 sequences each; this 500-sequence threshold is indicated with a dashed vertical line.

our sequence diversity estimates, which include both the naive and memory sequences, are not directly comparable to this previous estimate. Clonotype diversity estimates—which incorporate only V- and J-gene assignments, and the CDRH3 amino acid sequence—minimize the influence of somatic hypermutation, and are more suitable for comparison with previous estimates of naive repertoire diversity. The cohort-wide paired clonotype diversity using either estimator, under the same assumptions regarding light-chain diversity and random pairing, is estimated at 3 × 10^{15}—over three orders of magnitude greater than previously estimated for the naive repertoire.

Although it is known that convergent antibodies may arise from different individuals in response to immunological exposure, and a low frequency of CDRH3 sharing has previously been observed in healthy adult repertoires[9,15], the overall prevalence of repertoire sharing is unknown. For each combination of two or more subjects, we computed the frequency of shared clonotypes (Fig. 3a). Pairs of

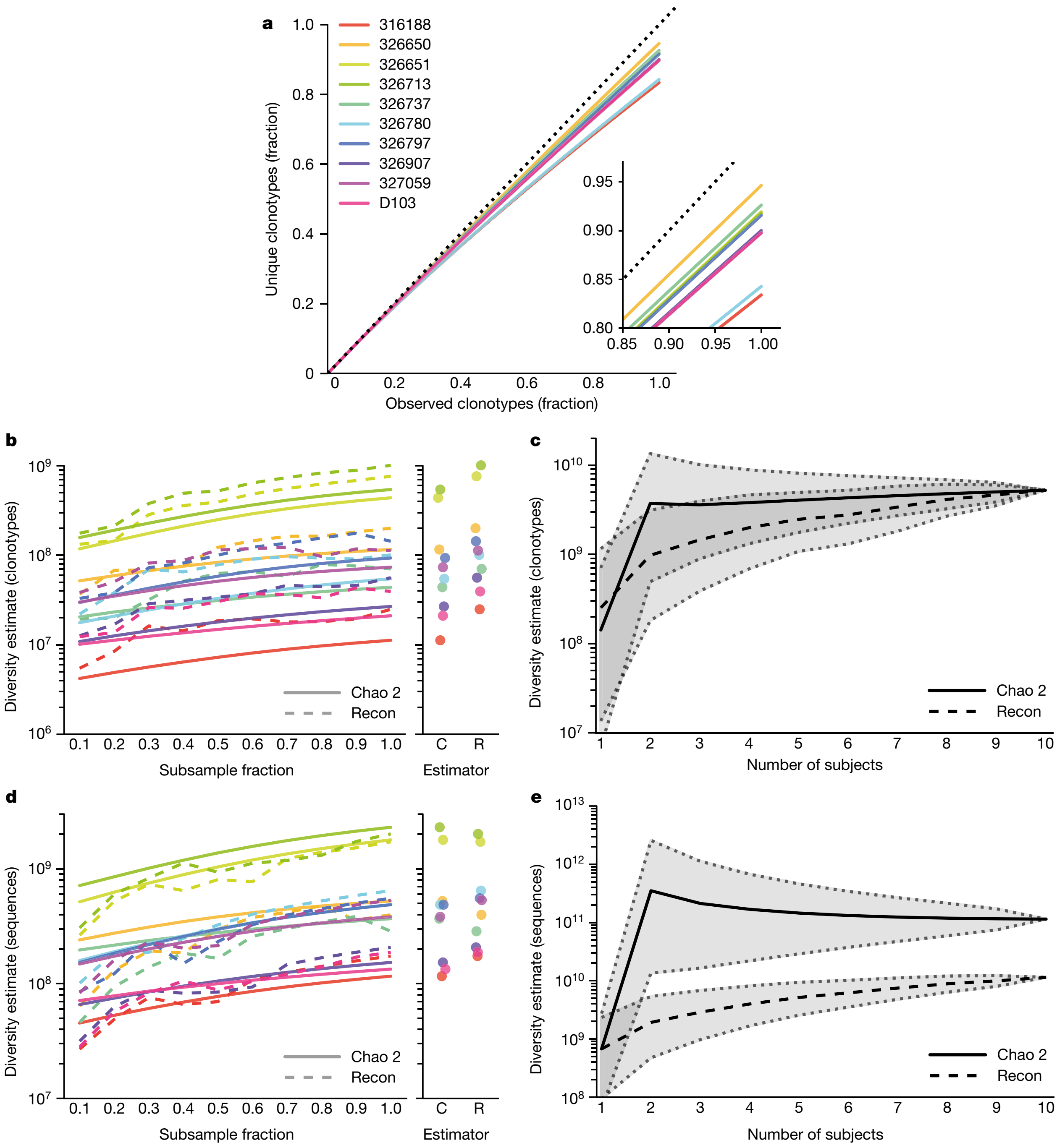

Fig. 2 | Clonotype and sequence diversity amongst the 10 subjects. **a**, Clonotype rarefaction curves for each subject. Lines represent the mean of 10 independent samplings, with the exception of the 1.0 fraction (which was sampled once). The dashed line represents a perfectly diverse sample. Inset is a close-up of the ends of the rarefaction curves. **b**, Estimates of total repertoire diversity per clonotype were computed for increasingly large fractions of the clonotype repertoire of each subject. Each line represents the mean of 10 random subsamplings without replacement (except for the 1.0 fraction). Chao 2 (C) estimates are shown in solid lines, Recon (R) estimates are shown in dashed lines. Subject colours are as in **a**. Maximum diversity (1.0 fraction of each subject) for each estimator is shown in the right panel. **c**, Overall cross-subject clonotype diversity of each possible combination of one or more subjects. The Chao 2 estimate is a solid line and the Recon estimate is a dashed line. Shaded regions indicate 95% confidence intervals. The confidence intervals in **c** are for different groupings of subjects, not for the estimators themselves. **d**, Estimates of total sequence repertoire diversity were computed for increasingly large fractions of the sequence repertoire of each subject. Each line represents the mean of 10 random subsamplings without replacement (except for the 1.0 fraction, for which only a single calculation was made). Chao 2 estimates are shown in solid lines, Recon estimates are shown in dashed lines. Subject colours are as in **a**. Maximum diversity (1.0 fraction of each subject repertoire) for each estimator is shown in the right panel. **e**, Overall cross-subject nucleotide sequence diversity of each possible combination of one or more subjects. The Chao 2 estimate is a solid line and the Recon estimate is a dashed line. Shaded regions indicate 95% confidence intervals. Confidence intervals are as in **c**.

subjects shared—on average—0.95% of their respective clonotypes, and 0.022% of clonotypes were shared by all ten subjects. We next used two approaches to quantify the expected frequency of clonotype sharing by chance. Hypergeometric distributions, based on cohort-wide clonotype diversity (Chao 2) and the number of unique clonotypes for each subject, indicated a low likelihood that the observed sharing was due to chance (8.8×10^{-6}, Bonferroni-corrected $P = 0.05$ is 1.1×10^{-3}). We also generated synthetic antibody sequences using IGoR[16] to determine

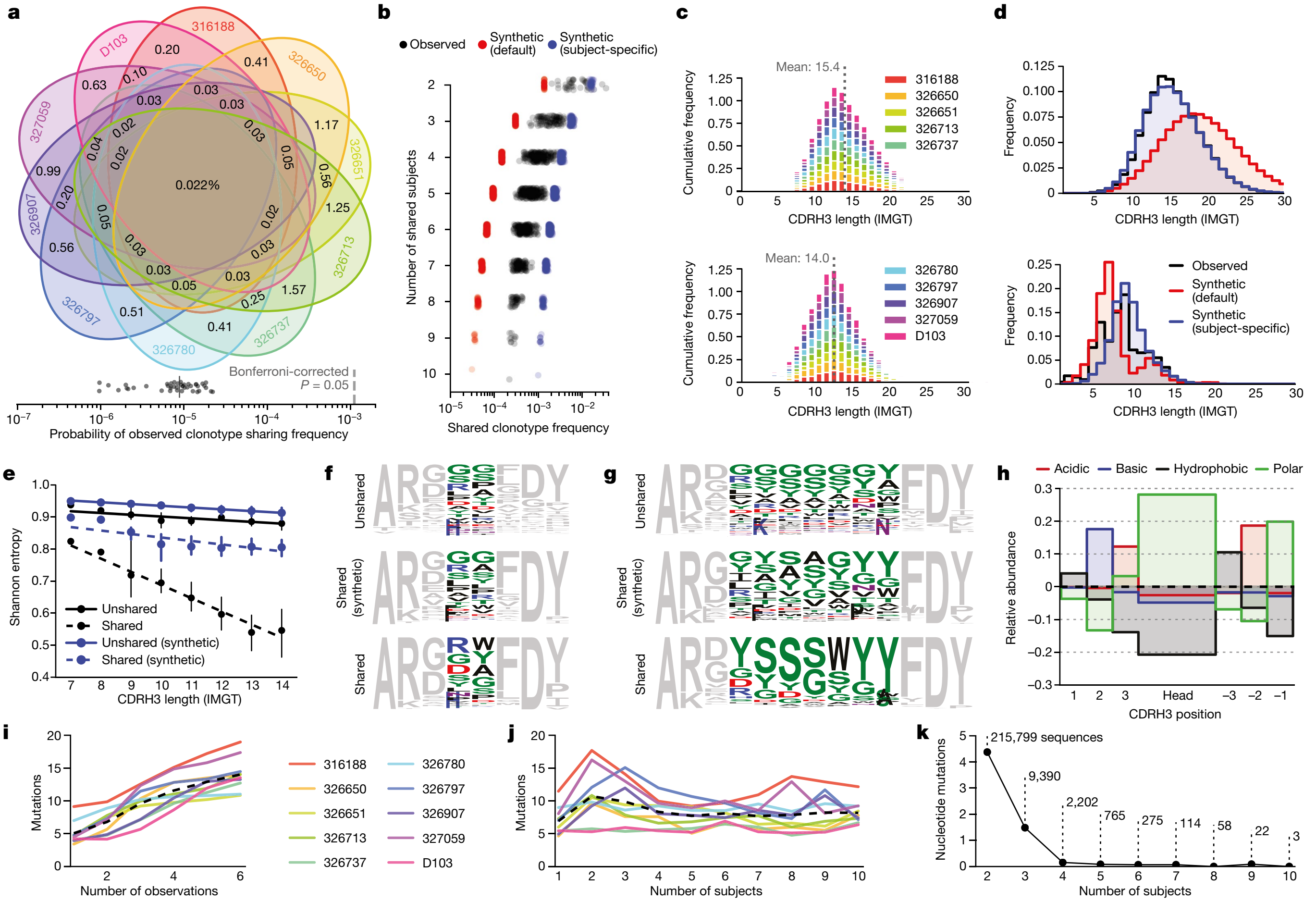

Fig. 3 | Shared clonotypes and sequences amongst the 10 subjects. **a**, Venn diagram of shared clonotype frequency. **b**, Shared clonotype frequency between subject groups. Points represent different group combinations. Observed sequences (black), synthetic sequences generated with IGoR's default model (red) and sequences generated with subject-specific models (blue) are shown. **c**, Distribution of CDRH3 lengths for clonotypes found in one biological replicate (top) or all six biological replicates (bottom). CDRH3 length is defined using IMGT numbering. The colour key legend is split to maintain legibility; data for all subjects are present in both plots. **d**, Distribution of CDRH3 length for unshared clonotypes (top) or clonotypes shared by the majority of subjects (bottom). Observed sequences (black), default model (red) and subject-specific model (blue) synthetic sequences are shown. **e**, Per position Shannon entropy of the CDRH3 head regions of unshared (solid) or majority-shared (dashed) clonotypes. Points indicate the mean, whiskers indicate the 95% confidence interval, and lines represent the linear best fit. **f**, **g**, Sequence logos of the CDRH3s encoded by observed unshared clonotypes, observed majority-shared clonotypes and synthetic majority-shared clonotypes of length 8 (**f**) or 13 (**g**). Head-region amino acid colouring: polar amino acids (GSTYCQN) are green; basic amino acids (KRH) are blue; acidic amino acids (DE) are red; and hydrophobic amino acids (AVLIPWFM) are black. All torso residues are grey. **h**, Relative abundance of amino acid properties in the CDRH3s of majority-shared clonotypes. Abundances are normalized to the frequency in unshared clonotypes. **i**, Nucleotide mutations for singly observed or repeatedly observed clonotypes. Coloured lines indicate the mean for each subject; dashed black line indicates the mean of all subjects. **j**, Nucleotide mutations for shared or unshared clonotypes. Coloured lines indicate the mean for each subject; dashed black line indicates the mean of all subjects. **k**, Mutation frequency of nucleotide sequences shared by two or more subjects. Points indicate mean mutation frequency. The number of unique nucleotide sequences in each shared group is shown.

the expected frequency of clonotype sharing due to coincident V(D)J recombination. Synthetic sequence sets were generated using three different recombination models: (1) IGoR's default model, inferred from unproductive antibody rearrangements and thus focused only on parameters related to V(D)J recombination; (2) subject-specific recombination models inferred from unmutated sequences from each subject; and (3) a combined-subject recombination model inferred from a pool of unmutated sequences drawn from all subjects. For each model, 10 batches of 10^8 sequences were generated, for a total of 3 billion synthetic sequences. In the sequence sets generated with IGoR's default model, clonotype sharing was sevenfold lower than in human repertoires (0.0032%; Fig. 3b), which indicates that coincident V(D)J recombination alone is not sufficient to explain the observed sharing. The subject-derived synthetic sequence sets showed much more sharing (0.1% and 0.16%, respectively; Fig. 3b, Extended Data Fig. 8). In addition to containing information about V(D)J recombination, the subject-derived models also implicitly encode information about the selection processes involved in B cell development. The increased frequency of clonotype sharing in subject-derived synthetic datasets indicates that the sieving effect of B cell development produces naive repertoires that are more similar than recombination alone would be expected to produce. Combined with our observation that naive-enriched repertoires are more similar to each other than are class-switched repertoires (Fig. 1h), a model emerges in which individual repertoires are very dissimilar after V(D)J recombination, are homogenized during B cell development and become increasingly individualized following differential responses to immunological exposure.

The length distributions of CDRH3s in unique and repeatedly observed clonotypes were similar, whereas short CDRH3s were much more common in shared clonotypes (Fig. 3c, d). The skew towards short CDRH3s in the shared population is probably due to the increased probability of similar recombination events among shorter CDRH3s. By contrast, repeatedly observed clonotypes are more often the result of clonal expansion, as evidenced by their increased mutation frequency (Fig. 3i). Shared nucleotide sequences showed a strong inverse relationship between mutation frequency and the number of shared subjects (Fig. 3k); almost all sequences shared by four or more subjects were unmutated. Thus, although coincident recombination infrequently produces identical antibody sequences, the likelihood of coincident recombination being linked to an identical set of somatic mutations is exceptionally low.

Antibody CDRH3s can be divided into two primary regions: the framework-proximal 'torso' and the more-variable 'head'[17,18]. When comparing size-matched samples of shared and unshared clonotypes, we noted less diversity in the head regions of shared clonotypes. Furthermore, head-region diversity in shared clonotypes was inversely related to length of CDRH3, which is a relationship that is not seen in unshared clonotypes or synthetic repertoires (Fig. 3e). This inverse relationship—along with the skewed distribution of CDRH3 lengths in shared clonotypes (Fig. 3d)—indicates that two distinct processes shape the shared clonotype population. The shortest shared CDRH3s encode head-region diversity, similar to unshared CDRH3s and synthetic CDRH3s of the same length (Fig. 3f). Thus, short CDRH3s are probably shared primarily owing to their lower CDRH3 diversity and concomitantly higher likelihood of independent generation by coincident recombination. By contrast, longer shared CDRH3s are less diverse than unshared or shared synthetic populations (Fig. 3g), and more commonly encode head regions that are enriched in polar, uncharged residues and lack hydrophobic residues (Fig. 3h). This implies the existence of a mechanism by which these shared clonotypes are selected or enriched after recombination, on the basis of the biochemical properties of their CDRH3 regions.

In summary, sequencing the circulating B cell population of ten individuals at unprecedented depth has revealed repertoires that are highly individualized and extremely diverse. We estimate cohort-wide repertoire diversity of approximately 5×10^9 unique heavy-chain clonotypes, and as many as 1×10^{11} unique heavy-chain sequences. This indicates that the paired antibody diversity available to the circulating repertoire is very large, perhaps in the region of 10^{16}–10^{18} unique antibody sequences. Despite this enormous diversity, clonotypes are shared more frequently than would be expected from coincident V(D)J recombination. Furthermore, we found that clonotype sharing is probably driven primarily by selection processes related to early B cell development rather than by convergent responses to common antigens. The possible clinical and diagnostic applications of sequencing the adaptive-immune repertoire are myriad—however, much work remains to be done before these applications can be implemented. The results described here are confined to circulating B cells, which represent a minority of the total B cell population. The repertories of circulating and tissue-resident B cells are known to differ[19], and these differences may influence overall repertoire diversity and sharing. Furthermore, we have studied only ten individuals from a limited age range (18–30 years) and geographical region at a single time point. Much larger cohorts—representing diverse ethnicities, geographies and ages—will be required to capture the true population-wide repertoire diversity. Nevertheless, large-scale sequencing of the human adaptive-immune repertoire holds immense potential. Our use of high-level antibody-feature frequencies to differentiate repertoires raises the possibility of identifying and classifying discrete repertoire perturbations associated with autoimmune disease and chronic infection. Furthermore, because the repertoire of adaptive-immune receptors encodes a comprehensive record of an individual's immunological encounters, leveraging large-scale sequencing of adaptive-immune receptors represents an appealing strategy for diagnosing infection or deconvoluting infection histories. Finally, the individuality of the baseline repertoire of each subject suggests that the personalization of vaccine delivery and therapeutic intervention may produce substantial benefits in the treatment and prevention of infectious diseases.

Online content

Any methods, additional references, Nature Research reporting summaries, source data, statements of data availability and associated accession codes are available at https://doi.org/10.1038/s41586-019-0879-y.

Received: 19 September 2017; Accepted: 22 November 2018;
Published online 21 January 2019.

1. Rajewsky, K. Clonal selection and learning in the antibody system. *Nature* **381**, 751–758 (1996).
2. Alberts, B. et al. *The Generation of Antibody Diversity* (Garland Science, New York, 2002).
3. Boyd, S. D. & Crowe, J. E. Jr. Deep sequencing and human antibody repertoire analysis. *Curr. Opin. Immunol.* **40**, 103–109 (2016).
4. Briney, B. & Burton, D. Massively scalable genetic analysis of antibody repertoires. Preprint at https://www.biorxiv.org/content/early/2018/10/19/447813 (2018).
5. Briney, B., Le, K., Zhu, J. & Burton, D. R. Clonify: unseeded antibody lineage assignment from next-generation sequencing data. *Sci. Rep.* **6**, 23901 (2016).
6. Morbach, H., Eichhorn, E. M., Liese, J. G. & Girschick, H. J. Reference values for B cell subpopulations from infancy to adulthood. *Clin. Exp. Immunol.* **162**, 271–279 (2010).
7. Morisita, M. Measuring of the dispersion of individuals and analysis of the distributional patterns. *Mem. Fac. Sci. Kyushu Univ. Ser. E* **2**, 5–235 (1959).
8. Horn, H. S. Measurement of 'overlap' in comparative ecological studies. *Am. Nat.* **100**, 419–424 (1966).
9. Setliff, I. et al. Multi-donor longitudinal antibody repertoire sequencing reveals the existence of public antibody clonotypes in HIV-1 infection. *Cell Host Microbe* **23**, 845–854 (2018).
10. Chao, A. Estimating the population size for capture–recapture data with unequal catchability. *Biometrics* **43**, 783–791 (1987).
11. Kaplinsky, J. & Arnaout, R. Robust estimates of overall immune-repertoire diversity from high-throughput measurements on samples. *Nat. Commun.* **7**, 11881 (2016).
12. Chao, A. & Chiu, C.-H. *Nonparametric Estimation and Comparison of Species Richness* https://doi.org/10.1002/9780470015902.a0026329 (John Wiley & Sons, 2016).
13. Eren, M. I., Chao, A., Hwang, W.-H. & Colwell, R. K. Estimating the richness of a population when the maximum number of classes is fixed: a nonparametric solution to an archaeological problem. *PLoS ONE* **7**, e34179 (2012).
14. DeKosky, B. J. et al. In-depth determination and analysis of the human paired heavy- and light-chain antibody repertoire. *Nat. Med.* **21**, 86–91 (2015).
15. Arnaout, R. et al. High-resolution description of antibody heavy-chain repertoires in humans. *PLoS ONE* **6**, e22365 (2011).
16. Marcou, Q., Mora, T. & Walczak, A. M. High-throughput immune repertoire analysis with IGoR. *Nat. Commun.* **9**, 561 (2018).
17. Morea, V., Tramontano, A., Rustici, M., Chothia, C. & Lesk, A. M. Conformations of the third hypervariable region in the VH domain of immunoglobulins. *J. Mol. Biol.* **275**, 269–294 (1998).
18. Finn, J. A. et al. Improving loop modeling of the antibody complementarity-determining region 3 using knowledge-based restraints. *PLoS ONE* **11**, e0154811 (2016).
19. Briney, B. S., Willis, J. R., Finn, J. A., McKinney, B. A. & Crowe, J. E. Jr. Tissue-specific expressed antibody variable gene repertoires. *PLoS ONE* **9**, e100839 (2014).

Acknowledgements The authors thank all of the study subjects for their participation and the Genomic Services Laboratory at the HudsonAlpha Institute for Biotechnology for their sequencing expertise. This work was supported by the National Institute of Allergy and Infectious Diseases (Center for HIV/AIDS Vaccine Immunology and Immunogen Discovery, UM1AI100663 (D.R.B.); Center for Viral Systems Biology, U19AI135995 (B.B.)), the International AIDS Vaccine Initiative (IAVI) through the Neutralizing Antibody Consortium SFP1849 (D.R.B.), and the Ragon Institute of MGH, MIT and Harvard (D.R.B.).

Author contributions B.B. and D.R.B. planned and designed the experiments. B.B., A.I. and C.J. performed experiments. B.B. analysed data. B.B. and D.R.B. wrote the manuscript. All authors contributed to manuscript revisions.

Competing interests The authors declare no competing interests.

Additional information
Extended data is available for this paper at https://doi.org/10.1038/s41586-019-0879-y.
Supplementary information is available for this paper at https://doi.org/10.1038/s41586-019-0879-y.
Reprints and permissions information is available at http://www.nature.com/reprints.
Correspondence and requests for materials should be addressed to B.B. or D.R.B.
Publisher's note: Springer Nature remains neutral with regard to jurisdictional claims in published maps and institutional affiliations.

METHODS

No statistical methods were used to predetermine sample size. The experiments were not randomized and investigators were not blinded to allocation during experiments and outcome assessment.

Leukapheresis samples. Full leukopaks (three blood volumes) were obtained from ten human subjects (Hemacare). Samples were collected at Hemacare's Southern California donor centre. Sample collection was performed under a protocol approved by the Institutional Research Boards of Scripps Research and Hemacare. Informed consent was obtained from each subject. All subjects were healthy, HIV-negative adults between the ages of 18 and 30 with no reported acute illness in the 14 days before leukapheresis. The subject pool was gender-balanced and evenly divided between African-American and Caucasian individuals (ethnicity was self-reported; Extended Data Table 1). Immediately upon receipt of the leukopak, peripheral blood mononuclear cells were purified by gradient centrifugation and cryo-preserved.

Amplification strategy and primer bias. We elected to use RNA as the template for antibody variable gene amplification, as this focuses our analysis on productive heavy-chain rearrangements and permits the use of amplification primers that anneal to the CH1 region (owing to the presence of an intron between the JH gene and CH region, the use of CH1 primers is not feasible when amplifying from DNA). The decision to use RNA has some inherent downsides, however—primarily the likelihood of overrepresentation of transcriptionally active B cells (namely, memory B cells and plasmablasts). It should be noted that the use of molecular barcodes, which enable identification and collapsing of reads that originate from the same RNA molecule, will not correct this problem. To reduce the influence of multiplexed primer sets on the resulting composition of antibody genes that are amplified, we designed an amplification strategy that limits the use of multiplexed primers that anneal to the V-gene region in an attempt to reduce primer bias during amplification. Following cDNA synthesis, second-strand synthesis was performed using multiplexed V-gene primers that encode an overhang that comprises a portion of the Illumina adapters required for next-generation sequencing. V-gene primers were then enzymatically removed before subsequent amplification of the antibody genes using the conserved overhang as the primer annealing site. Thus, the multiplexed V-gene primers were only used for a single round of amplification.

Antibody gene amplification. For each subject, total RNA was separately isolated from 6 aliquots of approximately 5×10^8 cryo-preserved peripheral blood mononuclear cells (RNeasy Maxi, Qiagen). For each RNA aliquot, antibody genes were amplified in triplicate (18 total samples per subject), with each of the technical replicates processed independently and starting with a separate aliquot of the RNA sample. To minimize the likelihood of crosscontamination between subjects, reverse transcription and PCR reactions for each subject were processed in isolation, such that samples from two different subjects were never in proximity during amplification reaction preparation. All primers[20] are listed in Extended Data Table 2. To increase the sequencer-perceived nucleotide diversity during each sequencing cycle, 'offsets' were added to the reverse-transcription and second-strand synthesis primers. Three sets of these primers were synthesized, with each set containing 2, 4 or 6 random nucleotides at the offset position (see Extended Data Table 2). These offsets stagger the conserved constant and framework regions and result in much higher diversity during each sequencing cycle, and minimize the required PhiX spike. cDNA synthesis was performed on 11 μl of RNA using 10 pmol of each primer in a 20-μl total reaction (SuperScript III, Thermo Fisher Scientific), using the manufacturer's protocol and the following thermal cycling program: 55 °C for 60 min, 70 °C for 15 min. Residual primers and dNTPs were degraded enzymatically (ExoSAP-IT, Thermo Fisher Scientific), according to the manufacturer's protocol. The entire enzyme-treated cDNA synthesis product was used in a 100-μl second-strand synthesis reaction using 10 pmol of each primer (HotStarTaq Plus, Qiagen) using the following thermal cycling protocol: 95 °C for 5 min, 55 °C for 30 s, 72 °C for 10 min. Residual primers and dNTPs were again degraded enzymatically (ExoSAP-IT) and dsDNA was purified using 0.8 volumes of SPRI beads (AmpureXP, Beckman Coulter Genomics) and eluted in 50 μl of water. Antibody genes were amplified using 40 μl of eluted dsDNA and 10 pmol of each primer in a 100-μl total reaction volume (HotStarTaq Plus), using the following thermal cycling program: 95 °C for 5 min; 25 cycles of: 95 °C for 30 s, 58 °C for 30 s, 72 °C for 2 min; 72 °C for 10 min. DNA was purified from the PCR reaction product using 0.8 volumes of SPRI beads (AmpureXP) and eluted in 50 μl of water. Subsequently, 10 μl of the eluted PCR product was used in a final indexing PCR (HotStarTaq Plus) using 10 pmol of each primer in 100-μl total reaction volume and using the following thermal cycling program: 95 °C for 5 min; 10 cycles of: 95 °C for 30 s, 58 °C for 30 s, 72 °C for 2 min; 72 °C for 10 min. PCR products were purified with 0.7 volumes of SPRI beads (SPRIselect, Beckman Coulter Genomics) and the entire set of samples from a single subject was eluted in a single 120-μl volume of water.

Sequencing. SPRI-purified sequencing libraries were initially quantified using fluorometry (Qubit, Thermo Fisher Scientific) before size determination using a Bioanalyzer (Agilent 2100). Libraries were requantified using qPCR (KAPA Biosystems) before sequencing on an Illumina HiSeq 2500 using 2 × 250-bp Rapid Run chemistry.

Raw sequence processing. Raw paired FASTQ files were quality checked with FASTQC (www.bioinformatics.babraham.ac.uk/projects/fastqc/). Because the 5′ end of each paired read encodes the unique molecular identifier (UMI), reads were quality trimmed only at the 3′ end using Sickle (www.github.com/najoshi/sickle), using a window size of 0.1 times the length of the read, minimum average window quality score of 20, and a minimum read length after trimming of 50 nucleotides. Because UMIs are located on the 'outside' of the gene-specific primers used for amplification (see Extended Data Fig. 1b), primer trimming was delayed until after UMI processing. Processed reads were quality checked again using FASTQC, and paired reads were merged with PANDAseq using the default (simple_bayesian) merging algorithm[21].

Molecular barcodes. Although sequencing libraries were constructed to encode molecular barcodes on both ends of the amplicon, we observed low-level PCR recombination[22] that produced 'barcode swapping', causing the frequency of these amplification artefacts to be amplified. In essence, a partial amplification product—composed of a CDRH3 and an incomplete VH gene—was able to prime a different antibody sequence and continue amplification, producing a hybrid VH gene. This hybrid amplicon encodes the 3′ molecular barcode from the primary antibody recombination and the 5′ molecular barcode from the second. The barcode swapping creates a unique barcode pair, forcing the hybrid sequence to be binned and processed separately. To minimize the effects of such barcode swapping, we binned sequences using only the 3′ molecular barcode. Because the likelihood of UMI collisions was relatively high given the sequencing depth, the CDRH3 nucleotide sequences of each UMI bin containing more than one sequence were clustered at high identity (90%) and a consensus sequence was computed for each cluster. For UMI bins containing only a single sequence, the lone sequence was used as the representative for the respective UMI bin. Because our sequencing depth was approximately equal to the number of input cells (~3×10^8 sequencing reads from ~3×10^8 input B cells), the majority of UMI bins contained only a single sequencing read. As such, the UMIs were not used primarily for error correction, but as a means for correcting differential representation arising from stochastic or primer-driven amplification biases. Mutation frequencies in the IgM and IgG sequence populations (Extended Data Fig. 3) provide empirical evidence of a low amplification and sequencing error rate that corroborates sequencer-derived quality metrics.

Germline gene assignment and annotation. Adapters and V-gene amplification primers (used for second-strand synthesis) were removed using cutadapt[23]. cDNA synthesis primers, which anneal to the CH1 region, were not removed because this region is needed to determine the isotype. Sequences were annotated with abstar[4] and two output formats were generated: a comprehensive JSON-formatted output, which was imported into a MongoDB database; and a minimal CSV-formatted output, which is tabular and suitable for direct parsing or conversion to Parquet for querying on a Spark cluster.

Antibody clonotypes. Antibody clonotypes, defined as a collection of sequences that use the same V and J germline segments and encode an identical CDRH3 amino acid sequence, were used throughout this study to reduce the influence of sequencing or amplification error. Although collapsing the V or J regions to just the germline assignment removes the possibility of double-counting sequences that differ only by error(s) in the V- or J-gene region, it does not eliminate the effect of error in the CDRH3 sequence. To gauge the effect of sequencing and amplification error in CDRH3 on clonotype diversity, we collapsed sequences into clonotypes allowing either no mismatches in the CDRH3 amino acid sequence or a single mismatch in the CDRH3 sequence. The total number of one-mismatch clonotypes was lower than the number of zero-mismatch clonotypes by only 5.9% on average (3.4–9.5%), which is as expected when collapsing a sequence population that contains expanded antibody lineages (Extended Data Fig. 5), and indicates that CDRH3 sequencing errors do not contribute meaningfully to clonotype diversity. Thus, only zero-mismatch clonotypes were used for all further experiments using clonotypes.

Estimation of light-chain diversity relative to heavy chain diversity. Estimation of light-chain diversity is in some ways more complex than estimating heavy-chain diversity, owing to the relatively high frequency of coincidentally identical recombinations[14]. Rather than sequencing unpaired light chains and attempting to discern independent rearrangements from distinct copies of RNA derived from the same recombination event, we leveraged a novel dataset of paired antibody heavy and light chains to estimate the diversity of light chains relative to the diversity of heavy chains[14]. For each of the three subjects for which paired heavy- and light-chain sequencing data were available, we estimated the total richness using Chao 2 and Recon estimators. Each subject was sequenced in duplicate, and separated estimates were computed for each sequencing replicate. Because the sequencing depth was far lower in the paired dataset than in the large-scale experiment described here, we extrapolated the richness estimates so that the paired richness estimates were more comparable with the large-scale estimates. Although such an extrapolation may introduce a non-trivial amount of variance into the richness estimates, we believe that this provides the most accurate estimate of relative light-chain diversity that is currently available. Diversity estimates and the associated extrapolations can be found in Extended Data Fig. 7. The highest ratio of heavy-chain to light-chain richness (indicating the lowest diversity of light chains relative to heavy chains) was observed with the Chao 2 estimator (3.8×10^3). Conservatively, we rounded this ratio up to the nearest order of magnitude (10^4) when computing the total paired repertoire diversity estimates.

Generating synthetic repertoires based on a probabilistic model of V(D)J recombination. We created a total of 3 billion synthetic antibody sequences using IGoR[16] with one of three different approaches. First, we created 10 sequence batches—each containing 10^8 synthetic antibody sequences—using IGoR's default recombination model, which was inferred from unproductive antibody rearrangements. The reason for using unproductive rearrangements for inferring IGoR's default recombination model is that productive rearrangements are subject to a variety of selection processes during B cell maturation (negative selection of autoreactive clones, requirement for productive pairing with a light chain, and so on), whereas unproductive rearrangements are subject to none of these selection processes. Thus, a model inferred from unproductive rearrangements incorporates only information about the V(D)J recombination process. Second, we inferred subject-specific recombination models using 5×10^5 randomly selected IgM sequences that were entirely unmutated in the V-gene region. Ten synthetic sequence batches, each containing 10^8 sequences, were then generated—one batch per subject. Finally, we inferred a combined-subject recombination model using a pool of 5×10^5 umutated IgM sequences from all 10 subjects (5×10^4 sequences per subject, randomly selected from the sequences used to generate the subject-specific models). As with IGoR's default model, 10 separate batches of 10^8 synthetic sequences were generated with the combined-subject model. All synthetic sequences were processed in the same manner as the observed antibody sequences, except that the adapter trimming and UMI-based correction steps were not performed. Kullback–Leibler divergence between models or model 'events' was computed with the pygor package, which is distributed with IGoR (Extended Data Fig. 8).

Morisita–Horn similarity. Antibody sequences from each subject were reduced to only the V-gene, J-gene and CDRH3 length (and were randomly subsampled with replacement at sample sizes ranging from 10^1 to 10^7). The frequency of each V-gene, J-gene and CDRH3 length was computed, and the frequency distributions from two donors were used to compute the Morisita–Horn similarity index:

$$C_H = \frac{2\sum_{i=1}^{S} x_i y_i}{\left(\frac{\sum_{i=1}^{S} x_i^2}{X^2} + \frac{\sum_{i=1}^{S} y_i^2}{Y^2}\right) XY}$$

in which x_i is the number of times the V-gene, J-gene and CDRH3 length i is represented in one sample of size X; and y_i is the number of times the V-gene, J-gene and CDRH3 length i is represented in a second sample of size Y.

Rarefaction. For each subject, all unique clonotypes from each of the biological replicates were pooled. For varying sample sizes (ranging from 0.1 to 1.0 as a fraction of the total number of pooled clonotypes), samples were randomly drawn without replacement and the number of unique clonotypes in the sample was computed. For each sample size, a total of 10 independent samplings were performed, with the exception of the 1.0 fraction, which was only sampled once (as samplings of the entire dataset will always produce the same result).

Classification of repertoires by subject. Repertoires were classified using a one-versus-rest support-vector-machine classifier. Classifier training and evaluation were performed in Python using the scikit-learn framework. It is important to note that this classification was performed using only ten subjects and expanding the subject pool to thousands or millions of individuals, while maintaining classifier accuracy, would likely require much larger training datasets and/or the inclusion of additional sequence features to supplement the V-gene, J-gene and CDRH3 length. Additionally, because the repertoire of each subject will be altered by new immunological encounters and ongoing turnover in the naive B cell population, it is possible that these high-level sequence feature frequencies will change substantially over time.

Statistical calculations. Statistical calculations were performed in Python using SciPy (www.scipy.org) or Seaborn (seaborn.pydata.org).

Reporting summary. Further information on research design is available in the Nature Research Reporting Summary linked to this paper.

Code availability. Code used to produce the figures is available at www.github.com/briney/grp_paper. All code used for classification can be found at www.github.com/briney/grp_paper. Abstar is available at www.github.com/briney/abstar. Code for molecular barcode processing is available at www.github.com/briney/abtools.

Data availability

Sequence data that support the findings in this study are available at the NCBI Sequencing Read Archive (www.ncbi.nlm.nih.gov/sra) under BioProject number PRJNA406949. Raw and processed datasets are available at www.github.com/briney/grp_paper.

20. van Dongen, J. J. M. et al. Design and standardization of PCR primers and protocols for detection of clonal immunoglobulin and T-cell receptor gene recombinations in suspect lymphoproliferations: report of the BIOMED-2 Concerted Action BMH4-CT98-3936. *Leukemia* **17**, 2257–2317 (2003).
21. Masella, A. P., Bartram, A. K., Truszkowski, J. M., Brown, D. G. & Neufeld, J. D. PANDAseq: paired-end assembler for Illumina sequences. *BMC Bioinformatics* **13**, 31 (2012).
22. Meyerhans, A., Vartanian, J. P. & Wain-Hobson, S. DNA recombination during PCR. *Nucleic Acids Res.* **18**, 1687–1691 (1990).
23. Martin, M. Cutadapt removes adapter sequences from high-throughput sequencing reads. *EMBnet J.* **17**, 10–12 (2011).
24. Rogers, T. F. et al. Zika virus activates de novo and cross-reactive memory B cell responses in dengue-experienced donors. *Sci. Immunol.* **2**, eaan6809 (2017).

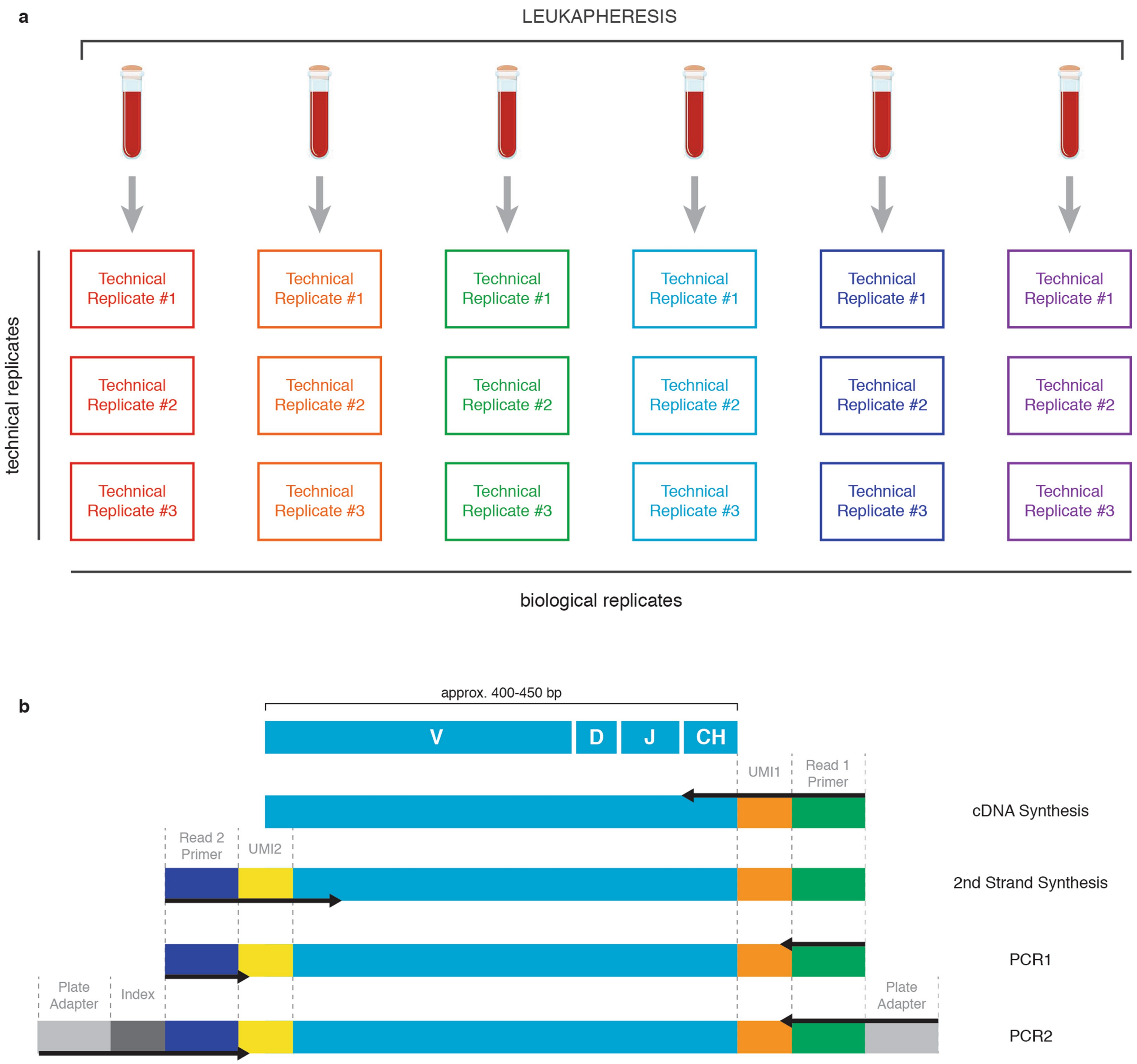

Extended Data Fig. 1 | Nearly full-length antibody gene amplification from biological and technical replicate samples. a, Schematic of biological and technical replicate samples. Biological replicates (columns) are derived from distinct cell aliquots, so identical clonotypes or sequences found in multiple biological replicates must arise from different cells. Technical replicates (rows) were amplified using discrete RNA aliquots from a single-cell aliquot. **b**, Strategy for nearly full-length antibody heavy chains. Black arrows indicate primers. Primers in the cDNA synthesis step anneal to the heavy-chain constant region (CH) and add the first unique molecular identifier (UMI) and the Illumina read 1 primer annealing site. Primers in the second-strand synthesis step anneal to the framework 1 region of the variable gene and add a second UMI and the Illumina read 2 primer annealing site.

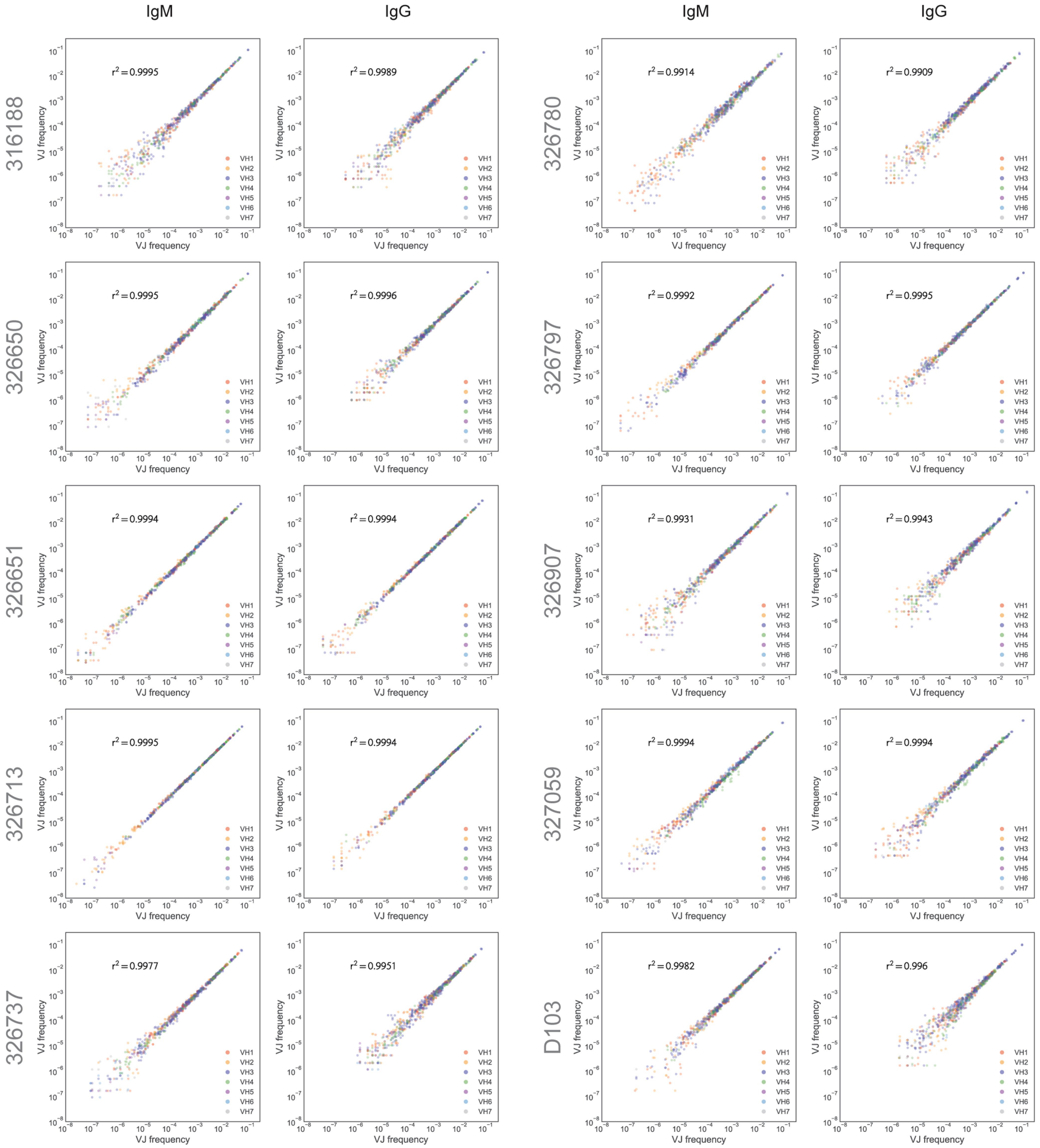

Extended Data Fig. 2 | V and J frequency correlations of technical and biological replicates. For each subject, the frequency of V and J combinations was compared for technical replicates (left panels) or biological replicates (right panels). The coefficient of determination (r^2) is shown for each plot.

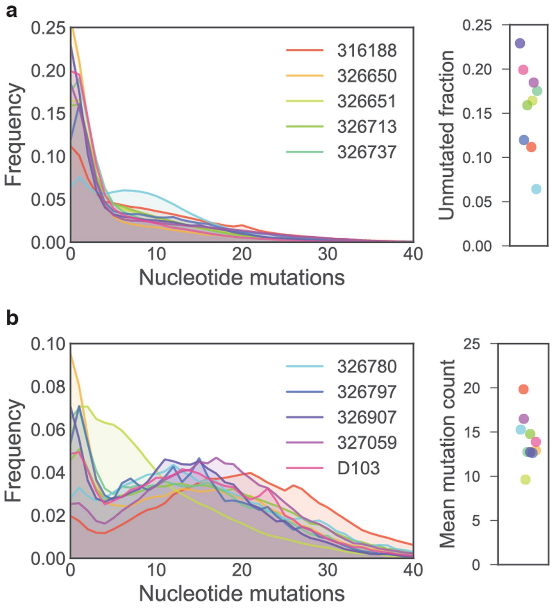

Extended Data Fig. 3 | Nucleotide mutation frequencies. a, The distribution of nucleotide mutations in sequences that encode IgM are shown. On the right, the number of unmutated sequences containing no mutations in the variable-gene segment is also plotted. **b**, The distribution of nucleotide mutations in sequences that encode IgG are shown. On the right, the mean mutation frequency for the IgG population of each subject is shown. Each line represents a single subject. For legibility, the legend is split between the two plots. Although only five subjects are shown in the legend of each plot, data from all ten subjects is present in each plot.

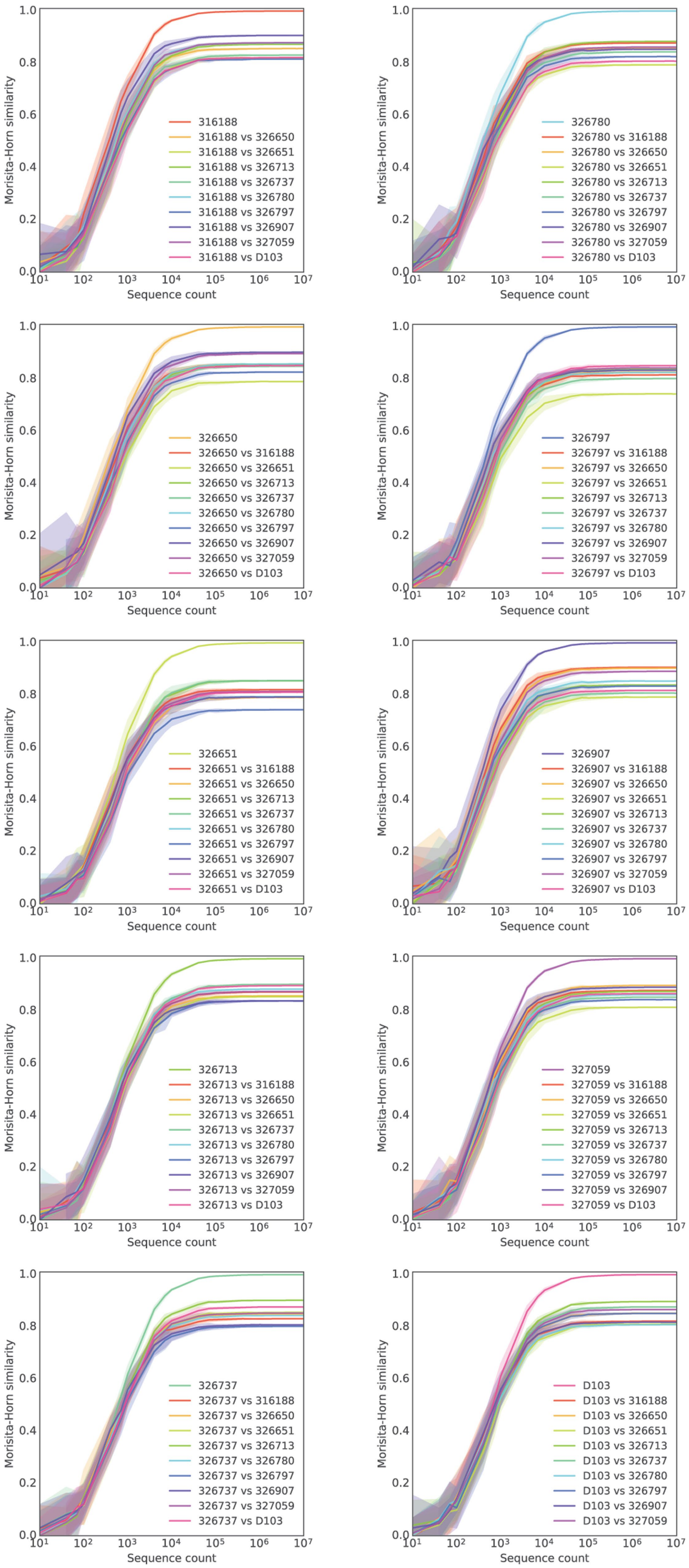

Extended Data Fig. 4 | Cross-subject repertoire similarity. Pairwise Morisita–Horn similarity comparisons between each subject and all other subjects. Similarity was computed using the frequency of V-gene, J-gene and CDRH3 length combinations. Each line represents the mean of 20 independent repertoire samplings (with replacement). The shading surrounding the mean line indicates the 95% confidence interval.

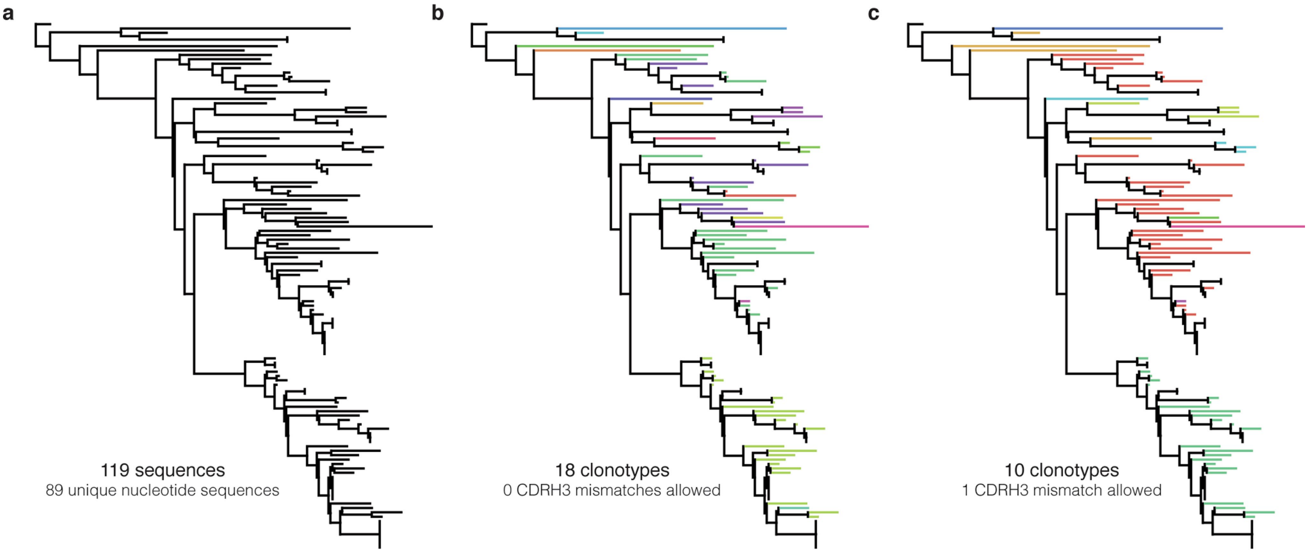

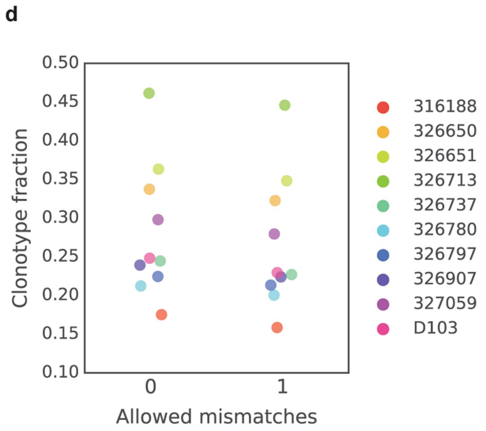

e

Subject	Clonotypes	
	0 mismatches	1 mismatch
316188	2,061,409	1,865,584
326650	8,295,298	7,935,396
326651	31,470,867	30,168,620
326713	41,809,045	40,405,491
326780	4,400,086	4,084,795
326797	8,483,433	8,009,495
326907	8,021,582	7,621,784
326907	3,236,704	3,030,208
327059	9,227,298	8,655,199
D103	2,914,936	2,696,342

Extended Data Fig. 5 | Collapsing sequences into clonotypes. a, To demonstrate the effect of collapsing an expanded clonal lineage into clonotypes, we selected a previously reported lineage of Zika-specific monoclonal antibodies isolated from the plasmablast population of an acutely infected patient[24]. Of 119 sequences, 89 were unique at the nucleotide level. **b**, Sequences encoding the same V gene, J gene and an identical CDRH3 amino acid sequence were collapsed into clonotypes, and the sequence phylogeny was coloured by clonotype. A total of 119 sequences were collapsed into 18 clonotypes. **c**, Sequences were collapsed into clonotypes, allowing a single mismatch in the CDRH3 amino acid sequence, and the sequence phylogeny was coloured by clonotype. A total of 119 sequences were collapsed into 10 clonotypes. **d**, The clonotype fraction (number of clonotypes divided by the total number of filtered sequences), when collapsing clonotypes while allowing zero or one mismatch in the CDRH3 amino acid sequence for each subject in this study. **e**, Number of total clonotypes recovered when allowing zero or one mismatch in the CDRH3 amino acid sequence for each subject in this study.

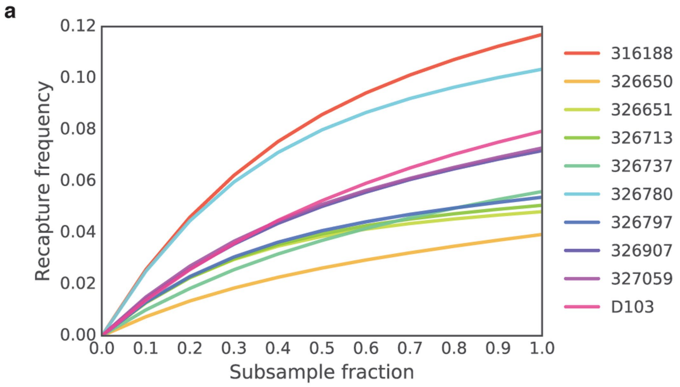

b

Subject	Recapture frequency									
	0.1	0.2	0.3	0.4	0.5	0.6	0.7	0.8	0.9	1.0
316188	0.026	0.046	0.062	0.075	0.086	0.094	0.101	0.107	0.112	0.117
326650	0.007	0.014	0.019	0.023	0.026	0.029	0.032	0.035	0.037	0.039
326651	0.013	0.023	0.03	0.035	0.039	0.041	0.044	0.045	0.047	0.048
326713	0.013	0.023	0.03	0.035	0.04	0.043	0.045	0.047	0.049	0.051
326737	0.01	0.018	0.026	0.032	0.037	0.042	0.046	0.049	0.053	0.056
326780	0.025	0.045	0.06	0.071	0.08	0.087	0.092	0.096	0.1	0.103
326797	0.013	0.023	0.031	0.036	0.041	0.044	0.047	0.05	0.052	0.054
326907	0.014	0.026	0.036	0.044	0.05	0.056	0.061	0.065	0.069	0.072
327059	0.015	0.027	0.037	0.045	0.051	0.056	0.061	0.065	0.069	0.073
D103	0.014	0.026	0.036	0.045	0.052	0.059	0.065	0.07	0.075	0.079

Extended Data Fig. 6 | Capture–recapture frequency. a, Recapture frequency for each subject. Lines represent the mean of 10 random samplings (without replacement) for all subsample fractions except compete sampling (1.0). **b**, Mean recapture frequency for each subsample fraction.

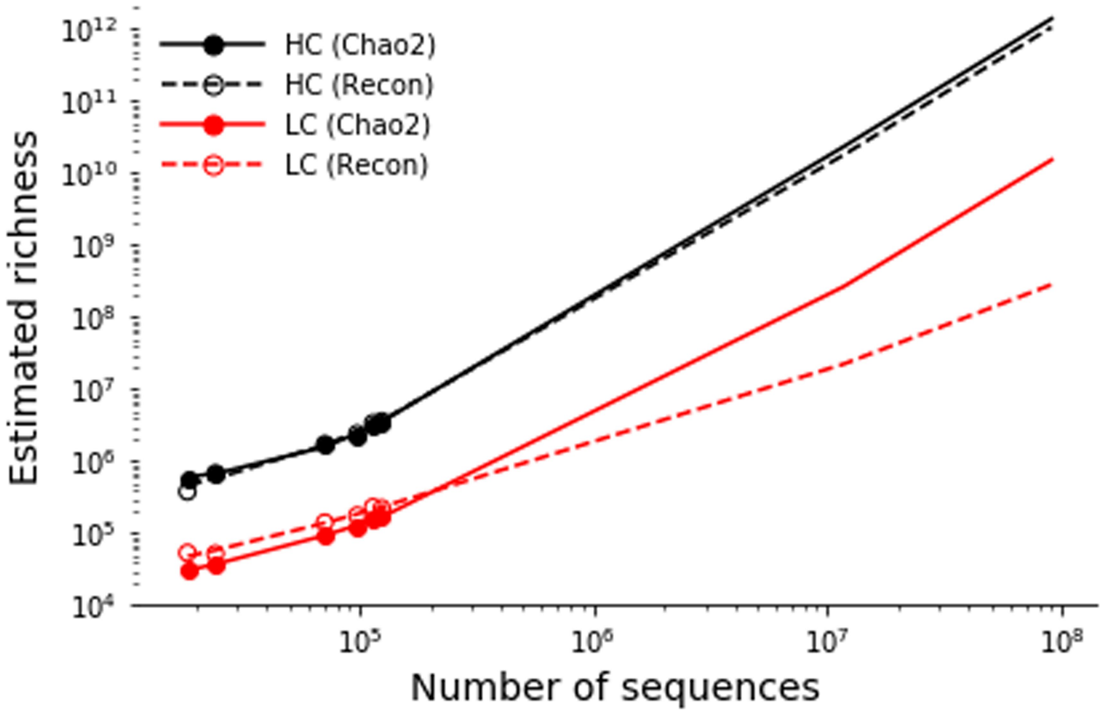

Extended Data Fig. 7 | Relative light-chain diversity estimation. Using previously reported datasets of paired heavy and light antibody chains, clonotype diversity was estimated for heavy and light chains using both Chao 2 and Recon estimators. Estimates are shown in filled or unfilled points. Lines indicate the least-squares polynomial best fit (degree = 2) and is extrapolated to include both the lowest (1.17×10^8) and highest (9.06×10^8) number of UMI-corrected sequences from the 10 sequenced subjects.

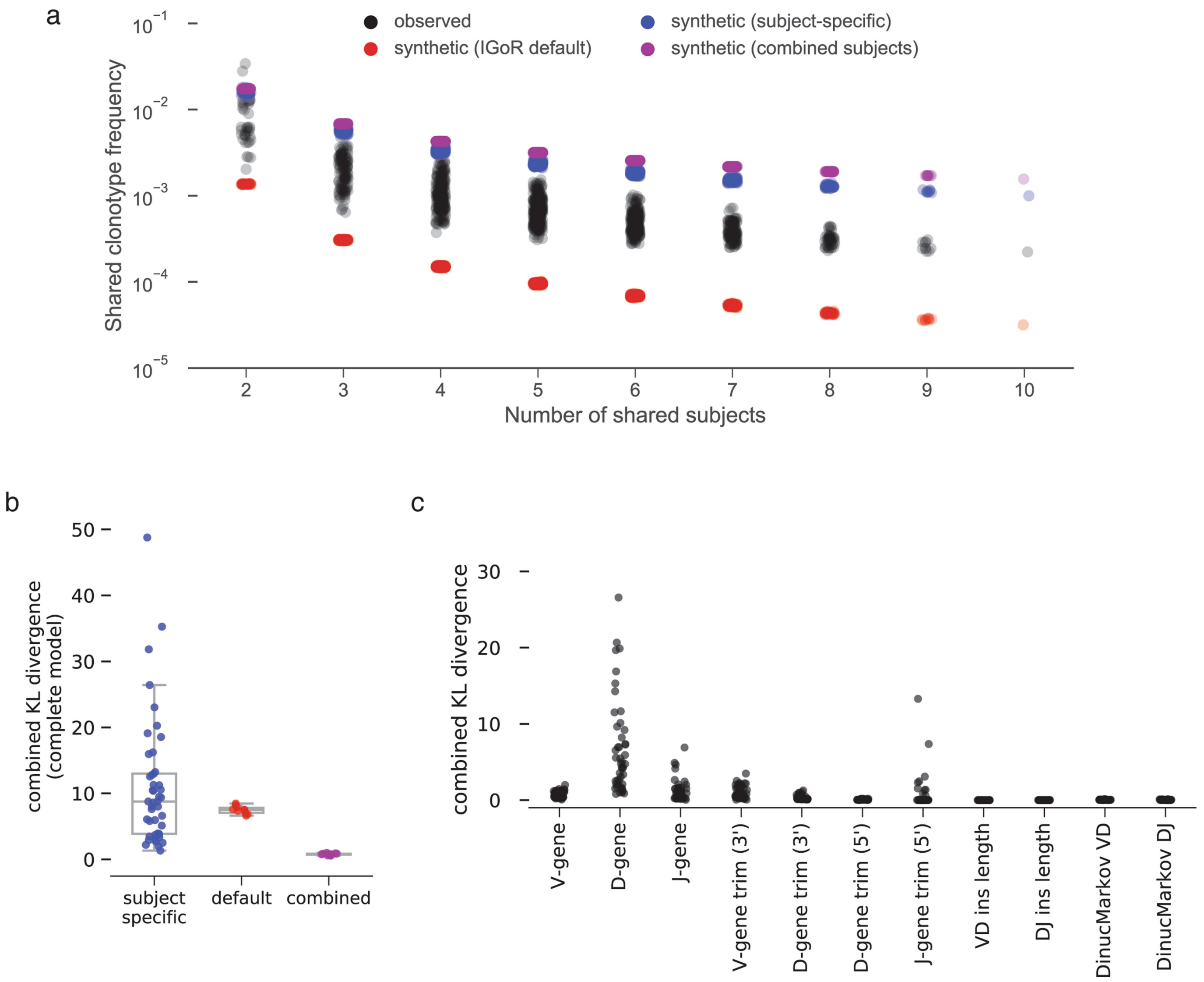

Extended Data Fig. 8 | Variance between inferred V(D)J recombination models. a, Frequency of clonotype sharing between observed human subjects (black), synthetic datasets generated with IGoR's default recombination model (red), synthetic datasets generated with subject-specific recombination models (blue) or synthetic datasets generated with a combined-subject recombination model (purple). **b**, Combined Kullback–Leibler divergence (KL divergence) between pairs of subject-specific models (blue), between subject-specific models and IGoR's default model (red), or between subject-specific models and the combined-subject model (purple). **c**, Combined KL divergence between pairs of subject-specific models, separated by event type.

Extended Data Table 1 | Demographic information and sequencing statistics per subject

Subject	Age	Gender	Blood Type	Ethnicity	Raw reads	Consensus sequences	Clonotypes	
							0 mismatch	1 mismatch
316188	30	female	A-POS	AA	320,844,194	11,767,640	2,061,409	1,865,584
326650	18	female	O-POS	C	218,356,368	24,592,893	8,295,298	7,935,396
326651	19	male	O-POS	AA	298,965,776	86,637,579	31,470,867	30,168,620
326713	25	female	O-POS	AA	228,526,194	90,598,768	41,809,045	40,405,491
326780	29	male	O-NEG	C	295,183,125	17,991,497	4,400,086	4,084,795
326797	21	female	A-POS	C	341,880,369	39,963,919	8,483,433	8,009,495
326907	29	male	AB-POS	C	275,955,787	35,726,036	8,021,582	7,621,784
326907	29	female	O-NEG	AA	267,970,240	13,528,917	3,236,704	3,030,208
327059	26	male	B-POS	AA/C	332,209,280	30,967,338	9,227,298	8,655,199
D103	25	male	O-NEG	C	322,781,254	11,746,606	2,914,936	2,696,342

All ethnicities are self-reported. AA, African-American; C, Caucasian.

Extended Data Table 2 | Primers used for antibody gene amplification

Name	Sequence	Step
IgM-RT	ACACTCTTTCCCTACACGACGCTCTTCCGATCTNNNNNNNNNNNN(NNNNNN)GGTTGGGGCGGATGCACTCC	RT
IgG-RT	ACACTCTTTCCCTACACGACGCTCTTCCGATCTNNNNNNNNNNNN(NNNNNN)SGATGGGCCCTTGGTGGARGC	RT
VH1-2SS	AGACGTGTGCTCTTCCGATCT(NNNNNN)GGCCTCAGTGAAGGTCTCCTGCAAG	2nd strand synthesis
VH2-2SS	AGACGTGTGCTCTTCCGATCT(NNNNNN)GTCTGGTCCTACGCTGGTGAACCC	2nd strand synthesis
VH3-2SS	AGACGTGTGCTCTTCCGATCT(NNNNNN)CTGGGGGGTCCCTGAGACTCTCCTG	2nd strand synthesis
VH4-2SS	AGACGTGTGCTCTTCCGATCT(NNNNNN)CTTCGGAGACCCTGTCCCTCACCTG	2nd strand synthesis
VH5-2SS	AGACGTGTGCTCTTCCGATCT(NNNNNN)CGGGGAGTCTCTGAAGATCTCCTGT	2nd strand synthesis
VH6-2SS	AGACGTGTGCTCTTCCGATCT(NNNNNN)TCGCAGACCCTCTCACTCACCTGTG	2nd strand synthesis
R1-fwd	GTGACTGGAGTTCAGACGTGTGCTCTTCCGATC	PCR1
R1-rev	ACACTCTTTCCCTACACGACG	PCR1
R2-fwd	CAAGCAGAAGACGGCATACGAGAGATCGGTCTCGGCATTCCTGCTGAAGATXXXXXXGTGACTGGAGTTCAGACGTGTGCTCTTCCGATC	PCR2
R2-rev	AATGATACGGCGACCACCGAGATCTACACTCTTTCCCTACACGACG	PCR2

Regions in parentheses indicate offset positions. Random offset nucleotides are added in multiples of two. RT, reverse transcription; X, position of Illumina TruSeq indices.

nature research

Corresponding author(s): Bryan Briney, Dennis R. Burton

Reporting Summary

Nature Research wishes to improve the reproducibility of the work that we publish. This form provides structure for consistency and transparency in reporting. For further information on Nature Research policies, see Authors & Referees and the Editorial Policy Checklist.

Statistical parameters

When statistical analyses are reported, confirm that the following items are present in the relevant location (e.g. figure legend, table legend, main text, or Methods section).

n/a	Confirmed	
□	☒	The exact sample size (*n*) for each experimental group/condition, given as a discrete number and unit of measurement
□	☒	An indication of whether measurements were taken from distinct samples or whether the same sample was measured repeatedly
□	☒	The statistical test(s) used AND whether they are one- or two-sided *Only common tests should be described solely by name; describe more complex techniques in the Methods section.*
☒	□	A description of all covariates tested
□	☒	A description of any assumptions or corrections, such as tests of normality and adjustment for multiple comparisons
□	☒	A full description of the statistics including central tendency (e.g. means) or other basic estimates (e.g. regression coefficient) AND variation (e.g. standard deviation) or associated estimates of uncertainty (e.g. confidence intervals)
□	☒	For null hypothesis testing, the test statistic (e.g. *F*, *t*, *r*) with confidence intervals, effect sizes, degrees of freedom and *P* value noted *Give P values as exact values whenever suitable.*
☒	□	For Bayesian analysis, information on the choice of priors and Markov chain Monte Carlo settings
□	☒	For hierarchical and complex designs, identification of the appropriate level for tests and full reporting of outcomes
□	☒	Estimates of effect sizes (e.g. Cohen's *d*, Pearson's *r*), indicating how they were calculated
□	☒	Clearly defined error bars *State explicitly what error bars represent (e.g. SD, SE, CI)*

Our web collection on statistics for biologists may be useful.

Software and code

Policy information about availability of computer code

Data collection	N/A
Data analysis	abcloud 0.1.0, abstar 0.3.4, abtools 0.2.0, abutils 0.0.6, biopython 1.70, boto3 1.6.3, celery 4.1.0, ipython 6.2.1, jupyter-core 4.4.0, jupyterlab 0.32.1, matplotlib 2.1.2, natsort 5.2.0, numpy 1.14.2, pandas 0.22.0, paramiko 2.4.0, pymongo 3.6.1, python 3.6.4, scikit-bio 0.5.1, scipy 1.0.0, seaborn 0.8.1, weblogo 3.6.0

For manuscripts utilizing custom algorithms or software that are central to the research but not yet described in published literature, software must be made available to editors/reviewers upon request. We strongly encourage code deposition in a community repository (e.g. GitHub). See the Nature Research guidelines for submitting code & software for further information.

Data

Policy information about availability of data

All manuscripts must include a data availability statement. This statement should provide the following information, where applicable:

- Accession codes, unique identifiers, or web links for publicly available datasets
- A list of figures that have associated raw data
- A description of any restrictions on data availability

Sequence data that support the findings in this study are available at the NCBI Sequencing Read Archive (www.ncbi.nlm.nih.gov/sra) under BioProject number PRJNA406949. Raw and processed datasets, as well as code for data processing and figure generation, are available at www.github.com/briney/grp_paper.

Field-specific reporting

Please select the best fit for your research. If you are not sure, read the appropriate sections before making your selection.

☒ Life sciences ☐ Behavioural & social sciences ☐ Ecological, evolutionary & environmental sciences

For a reference copy of the document with all sections, see nature.com/authors/policies/ReportingSummary-flat.pdf

Life sciences study design

All studies must disclose on these points even when the disclosure is negative.

Sample size

Sample size was determined by estimating intra-subject repertoire differences using data from prior studies.

Data exclusions

No data were excluded

Replication

Multiple biological replicates (distinct cell aliquots) and technical replicates (duplicated processing of the same biological replicate) were analyzed for each subject.

Randomization

N/A. This study did not divide subjects into experimental groups.

Blinding

N/A. Blinding was not relevant to this study, as subjects were not divided into experimental groups.

Reporting for specific materials, systems and methods

Materials & experimental systems

n/a	Involved in the study
☒	☐ Unique biological materials
☒	☐ Antibodies
☒	☐ Eukaryotic cell lines
☒	☐ Palaeontology
☒	☐ Animals and other organisms
☐	☒ Human research participants

Methods

n/a	Involved in the study
☒	☐ ChIP-seq
☒	☐ Flow cytometry
☒	☐ MRI-based neuroimaging

Human research participants

Policy information about studies involving human research participants

Population characteristics

All subjects were healthy adults between the ages of 18-35. The subject cohort contained an balanced mix of gender (5 males and 5 females) and contained equal numbers of self-identified Caucasian and African-American subjects. Additionally, all subjects reported no acute illness within the 14 days prior to leukapheresis.

Recruitment

Subjects were recruited by our clinical partner (HemaCare, Inc). Researchers involved in the study did not participate in subject recruitment beyond establishment of exclusion criteria. All samples were de-identified prior to delivery.